

## A THERMAL INTERPRETATION OF THE X-RAY SPECTRA OF QUASARS, ACTIVE GALACTIC NUCLEI, AND CYGNUS X-1

P. MÉSZÁROS<sup>1</sup>

Harvard-Smithsonian Center for Astrophysics  
 Received 1983 May 11; accepted 1983 June 28

### ABSTRACT

We show that spherically accreting black hole models emitting bremsstrahlung radiation provide an excellent fit to the observed X-ray spectrum of typical active galactic nuclei, as well as of 3C 273 and Cygnus X-1. The spectral slope remains approximately constant under changes of luminosity, as required by observations. Only one parameter,  $T_{\max}$ , is needed for the fit.

*Subject headings:* black holes — galaxies: nuclei — gamma rays: general — quasars — X-rays: sources

### I. INTRODUCTION

A very large number of high-energy sources, currently believed to be black holes, emit most of their radiation in the range from about 1 keV up to about a few MeV. Among these are QSOs, active galactic nuclei (AGNs), and galactic sources such as Cyg X-1, Cir X-1, V861 Scorpii, and LMC X-3. In general, ignoring other wavelength ranges, the X-ray spectrum is remarkably power-law like, sometimes with a high energy turnover. Recent reviews of the data and their interpretation have been given by, e.g., Rothschild (1981) and Mushotzky (1983). Several mechanisms have been studied to explain this remarkably constant spectrum (e.g., Lightman 1981 for a review), among which are (1) Comptonization by thermal electrons and (2) synchro-Compton, or Comptonization by relativistic electrons. We investigate here a third mechanism: (3) bremsstrahlung by thermal electrons at different temperatures.

There are strong reasons for bringing forward the bremsstrahlung mechanism. One of these is that it has the desirable property of maintaining a constant spectral slope during changes of luminosity, as observed in extragalactic sources. Also, to fit the spectrum of most objects, the variation of a simple parameter  $T_{\max}$  (instead of two) may be sufficient, and this parameter can be reasonably estimated from theory, instead of being arbitrary. Finally, a thermal mechanism is the simplest available under most circumstances and therefore worth exploring in some detail before going to more complicated interpretations. Here, we discuss the integrated, optically thin spectrum from different spherical accretion models, emphasizing the simplest version, in which  $\rho \propto r^{-3/2}$  and  $T \propto r^{-1}$  are approximately valid.

<sup>1</sup>Visiting Scientist, Smithsonian Astrophysical Observatory, supported in part by NASA grant NAGW 246; on leave from Max-Planck-Institut für Physik und Astrophysik MPA, Garching.

### II. BREMSSTRAHLUNG SPECTRA

We are interested in the range of temperatures from approximately 1 keV to approximately 5 MeV, and the calculations that exist are scattered throughout the literature, none of them covering the whole range we need. The best known regime is the low-energy one,  $kT \lesssim 500$  keV, where calculations have gone beyond the Born approximation, to include non-dipole and relativistic corrections. In particular, the electron-proton and electron-electron calculations of Gluckstern *et al.* (1953; cf. also Kylafis and Lamb 1982), Quigg (1968*a, b*) and Maxon (1972) agree with each other in this range. In the range  $kT > 511$  keV, the *e-p* bremsstrahlung has been calculated numerically in the Born approximation by Górecki and Kluźniak (1981), while calculations of the *e-e* bremsstrahlung have been made by Zdziarski (1983). These high-energy calculations do not match quite smoothly to those in the low-energy range, as is to be expected, since different approximations are involved. Discrepancies of the order of 10% to 30% occur where they overlap. To achieve a smooth transition, we introduced a correction factor in the range  $0.2 \leq (kT_e/m_e c^2) \leq 1$ , which bridges the two regimes. A unified set of spectral emissivity curves  $\epsilon_E(E)$  (ergs cm<sup>-3</sup> s<sup>-1</sup> ergs<sup>-1</sup>) is given in Figure 1, giving separately the *e-p*, *e-e*, and total contributions. As has been stressed before, above about 100 keV the *e-e* contribution is significant, becoming approximately twice the *e-p* contribution at frequencies  $\geq kT_e$  for  $kT_e \geq 0.5$  MeV.

We now apply this emissivity to models of spherically accreting black holes. In the simplest models, the gas is in free fall, so  $\rho \propto r^{-3/2}$ . The temperature behaves, over many decades in radius, as  $T_e \propto r^{-\alpha}$ . In particular, if  $(t_{\text{heat}}, t_{\text{cool}}) > t_{\text{infall}}$ , the adiabatic law is  $T \sim r^{-1}$ . Turbulent dissipation gives  $\alpha = 2$  if bremsstrahlung is the only cooling and  $t_{\text{cool}} < t_{\text{infall}}$ , since  $H \sim r^{-4}$ ,  $C \sim \rho^2 T^{1/2} \sim r^{-3} T^{1/2}$ , so  $T \sim r^{-2}$ . Here  $H$  and  $C$  are heating and cooling rates per cm<sup>2</sup>. If cyclotron cooling is

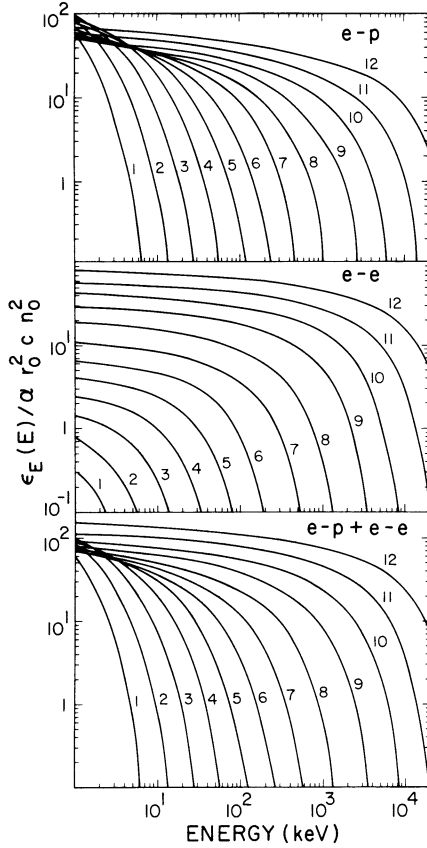


FIG. 1.—(upper) The  $e$ - $p$  bremsstrahlung spectrum  $\epsilon_E(E)$  (ergs  $\text{cm}^{-3} \text{s}^{-1} \text{ergs}^{-1}$ ), normalized by  $\alpha r_0^2 c n_0^2$ , where  $\alpha = (137)^{-1}$ ,  $r_0$  is electron radius, and  $n_0 = n_e = n_p$  is baryon density. The curves are in equal logarithmic steps of  $\log \theta = \log(kT/m_e c^2)$ , from  $\log \theta = -2.66$  to 10. Thus, the labels 1 to 12 correspond to  $kT = 1.11, 2.37, 5.11, 11.1, 23.7, 51.1, 111, 237, 511, 1110, 2370$ , and 5110 keV respectively. (middle) The same notation for  $e$ - $e$  bremsstrahlung. (lower) The sum of  $e$ - $p$  +  $e$ - $e$  contributions, for  $n_e = n_p = n_0$ .

included, this becomes  $T \sim r^{-\alpha}$ , with  $\alpha \sim 1$  (Mészáros 1975). If the heating efficiency is less than  $3 \times 10^{-1} - 10^{-2}$ , the power law can extend to the horizon without exceeding  $m_e c^2/k$ . Compton heating of non-dissipative infall (Ostriker *et al.* 1976; Cowie, Ostriker, and Stark 1978) would give  $H \sim \rho r^{-2} \sim r^{-7/2}$ ,  $C \sim \rho^2 T^{1/2} \sim r^{-3} T^{1/2}$ , and  $T \sim r^{-1}$ . Other freely falling spherical models, involving similar elements (Maraschi *et al.* 1979; Ipser and Price 1982) also lead approximately to  $T \sim r^{-\alpha}$ , with  $\alpha$  close to 1 near the region from which the hard X-ray spectrum arises. Recently, Mészáros and Ostriker (1983) have shown that, in spherically accreting black holes, one may have shocks, below which the electrons are heated to  $kT_e = \theta_2 m_e c^2$ , with  $\theta_2 \leq 1$ . The gas above the shock is freely falling, and subject to Compton heating (by photons  $\langle h\nu_\gamma \rangle$  arising from below the shock) and bremsstrahlung cooling. For moderate clumpiness, one has ( $t_{\text{cool}}, t_{\text{heat}}$ ) less than  $t_{\text{infall}}$ , leading to  $\rho \sim r^{-3/2}$  and  $T \sim T_{\text{max}}(r/r_s)^{-1}$ .

Here  $r_s$  is the shock radius ( $r_s < 50$  Schwarzschild units). The region below the shock, which produces the heating photons, is self-Comptonized, so that  $\langle h\nu_\gamma \rangle$  may be in the range from 1 to 3 times  $\theta_2 m_e c^2$ , i.e., 0.5–1.5 MeV. The Compton heating and cooling enter in the Kompaneets equation as  $(4kT - h\nu)$ , so  $kT_{\text{max}} \leq \langle h\nu_\gamma \rangle/4$ , giving  $130 \text{ keV} \leq kT_{\text{max}} \leq 400 \text{ keV}$ . In all the above models, the bulk of the 0.1–500 keV radiation would be due to the emission of the  $\rho \sim r^{-3/2}$ ,  $T \sim r^{-1}$  regions (or similar power laws).

As specific examples, we calculate here models with  $\rho \sim r^{-3/2}$  and  $T \sim T_{\text{max}}(r/r_s)^{-1}$ . This represents the case of the Mészáros and Ostriker (1983) model, but it also fits approximately some of the other spherical models. The total number of photons  $N_E$  per unit energy emitted by the flow between  $r_s$  and some large radius  $r_a$  (both in centimeters) is given by the integral

$$N_E = \int_{r_a}^{r_s} dr 4\pi r^2 \epsilon_E(n, T) E^{-1} \text{ photons s}^{-1} \text{ keV}^{-1}. \quad (1)$$

This spectrum will not be modified significantly by Comptonization if  $y_{\text{max}} = (4kT_{\text{max}}/m_e c^2)\tau_T^2 \ll 1$ . Since above the shock  $\tau_T < 2(Mc^2/L_{\text{Edd}})(r/2GMc^2)^{-1/2}$ , this implies  $\dot{M} \leq 10^{-1} c^{-2} L_{\text{Edd}}$  in terms of the Eddington luminosity. In nonshock spherical models,  $y_{\text{max}} \ll 1$  if  $\dot{M} < 10^{-2} c^{-2} L_{\text{Edd}}$ . Bremsstrahlung reabsorption is negligible at X-ray frequencies for these optical depths. Doppler effects and general relativistic corrections are neglected in equation (1), which may be adequate for  $r_s$  not too close to the horizon. The total emissivity  $\epsilon_E(n, T)$  includes both  $e$ - $p$  and  $e$ - $e$  contributions and depends on density as  $n_p n_e$  or  $n_e^2$  as well as on temperature  $T_e$ . The quantity  $\epsilon_E(E) = \epsilon_{ep}(E) + \epsilon_{ee}(E)$  is plotted in Figure 1c. For  $n_p = n_e = n_0 \propto r^{-3/2}$ , the  $n^2$  factor and the volume factor  $r^2$  give a net  $r^{-1}$  dependence, so that equal logarithmic intervals of  $r$  contribute equally to the luminosity, except for the temperature dependence. We have plotted in Figure 2 the integral (1) for  $kT_{\text{max}}$  between 51.1 keV and 5.11 MeV, or  $\theta_{\text{max}}$  between  $10^{-1}$  and 10 at logarithmic intervals. For  $n \sim r^{-3/2}$ , these integral photon spectrum curves can be obtained, aside from a constant, by adding the individual contributions of  $T$  up to  $T_{\text{max}}$ . It is seen that the general behavior is one of a power law at  $E \ll kT_{\text{max}}$  and an exponential dropoff at  $E$  greater than a few  $kT_{\text{max}}$ . Between the low-energy asymptote and the dropoff, the slope changes *very* slowly, over a transition region of more than two decades in frequency. The low-frequency asymptote is  $N_E \sim E^{-1.5}$ , and is *not* given by the asymptote of the Gaunt factor, which in the nonrelativistic region is  $\bar{g} \sim E^{-0.4}$ . It is given instead by the  $T^{-1/2}$  factor of the nonrelativistic emissivity  $\epsilon_E \propto n^2 T^{-1/2} e^{-E/kT}(r)$ . One can see that this asymptote is  $N_E^{\text{as}} \sim V \cdot \epsilon_E \cdot E^{-1} \sim r^3 n_0^2 T^{-1/2} e^{-E/kT} E^{-1} \sim T^{-1/2} E^{-1} \sim r^{\alpha/2} E^{-1} \sim E^{-1/2} E^{-1} \sim E^{-3/2}$  (since the envelope is given by the

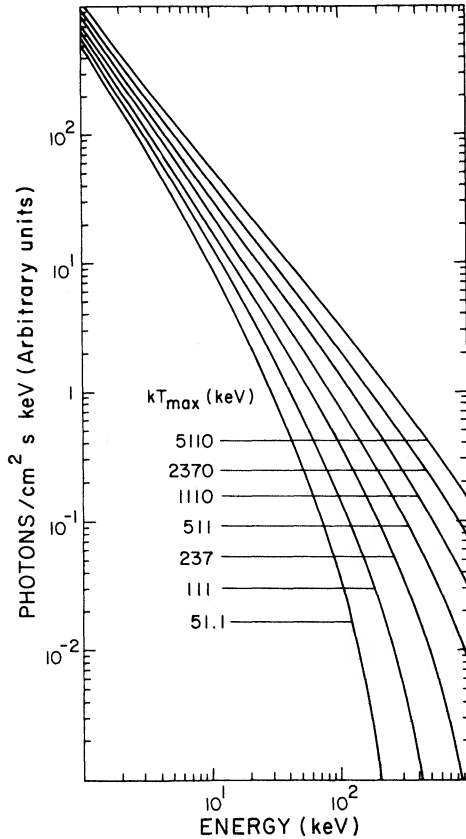


FIG. 2.—Theoretical photon number spectra obtained by integrating the bremsstrahlung emissivity over spherical accretion flows with  $\rho \sim r^{-3/2}$ ,  $T \sim T_{\max} r^{-1}$ , for different values of  $T_{\max}$ .

points with  $E \sim kT \sim r^{-\alpha}$ ). This is true for any power-law  $T \sim r^{-\alpha}$  with  $\alpha > 0$ . More exactly, in the nonrelativistic limit with  $T = T_0 r^{-\alpha}$

$$N_E^{\text{NR}} \propto \int_{\infty}^1 n^2 T^{-1/2} e^{-E/kT} E^{-1} r^2 dr$$

$$\propto \int_{\infty}^1 r^{-1+5\alpha} e^{-Ar^\alpha} E^{-1} dr, \quad (2)$$

where  $r$  is in units of  $r_3$ . Changing to the variable  $t = (2Ar^\alpha)^{1/2}$ , where  $A = E/kT_0$ , this becomes  $N_E^{\text{NR}} \propto A^{-3/2} \int_{(2A)^{1/2}}^{\infty} \exp(-t^2/2) dt$ . Calling  $x = (2A)^{1/2} = (2E/kT_0)^{1/2}$ , the integral is proportional to  $[1 - F(x)]$ , where  $F(x) = (2\pi)^{-1/2} \int_{-\infty}^x \exp(-t^2/2) dt$  is the error function. Thus

$$N_e^{\text{NR}} \propto x^{-3} [1 - F(x)] \quad (3)$$

in the nonrelativistic limit, which for  $x \rightarrow 0$  tends to  $x^{-3} \propto E^{-3/2}$  (see also Mészáros 1975; Mészáros and Silk 1977). The same nonrelativistic asymptote applies (in the region  $E \ll m_e c^2$  and  $E \ll kT_{\max}$ ) for integra-

tions extending into relativistic temperatures, as we are doing here. The nature of the slow turnover from  $E^{-1.5}$  to the exponential behavior is given, for  $kT_{\max} \leq 50$  keV, by the  $[1 - F(x)]$  factor of equation (3). For  $kT_{\max} \geq 50$  keV, the expression (3) is not valid, but a somewhat similar, gradual change from  $E^{-1.5}$  to  $e^{-E/kT_{\max}}$  is seen in the numerical integrations of Figure 2. For  $kT_{\max} > 0.5$  MeV, an initial, slight flattening from the  $E^{-1.5}$  behavior sets in before the slow steepening toward the exponential falloff. The remarkable thing is that, over a range of about two decades, where most X-ray observations are made, excellent power-law fits can be made to these spectra. The slope depends on the frequency window looked at and on the value of  $kT_{\max}$ , typical values being 1.6–1.7 for the photon number spectrum  $N_E$ .

### III. COMPARISON WITH OBSERVATIONS AND DISCUSSION

There is a very large body of information on the X-ray spectrum of active galactic nuclei, quasars, and Seyfert galaxies (see, e.g., Mushotzky 1983 for a recent review). Many of the observational data are in the 2–10 keV band, but a large amount of information also is known over a broader band of 2–165 keV from the *HEAO 1* experiment (e.g., Rothschild *et al.* 1983), as well as a number of other experiments. In particular, Rothschild *et al.* (1983) have presented data on a “mean” 2–165 keV AGN spectrum. We show this in Figure 3a (*points and error bars*) and superpose on this one of our theoretical spectra corresponding to  $kT_{\max} = 237$  keV. Without any particular optimization, the visual fit is seen to be extremely good over the whole range 2–165 keV. There could be some question about the last highest energy bin, but even this is within the given error bars. The slope obtained is 1.62, as observed.

Next, we consider the observed spectrum of 3C 273, using for the 2–20 keV range the *HEAO A-2* observations (Worrall *et al.* 1979), and in the 20–105 keV range the *HEAO 1* observations (Primini *et al.* 1979). The observational slope here is somewhat flatter, close to 1.5 over the 2–100 keV range. We superpose over the observed points and error bars a theoretical spectrum for  $kT_{\max} = 511$  keV (Fig. 3b). Again, without any particular optimization procedure, the fit is seen to be very good over the whole range.

Our final test object is the galactic black hole candidate Cyg X-1, for which we use the *HEAO 1* 10 keV to 6 MeV spectrum discussed by Rothschild (1981), shown in Figure 3c. At lower frequencies, spectral variations correlated with intensity changes have been reported. Most of the output of this object is, however, in the  $E > 10$  keV region, which is more stable. We superpose on the observed spectrum a theoretical curve for  $kT_{\max} = 237$  keV and find that it provides an excellent fit for the range from 10 keV up to 225 keV. Furthermore, it also goes through the three highest energy points positively

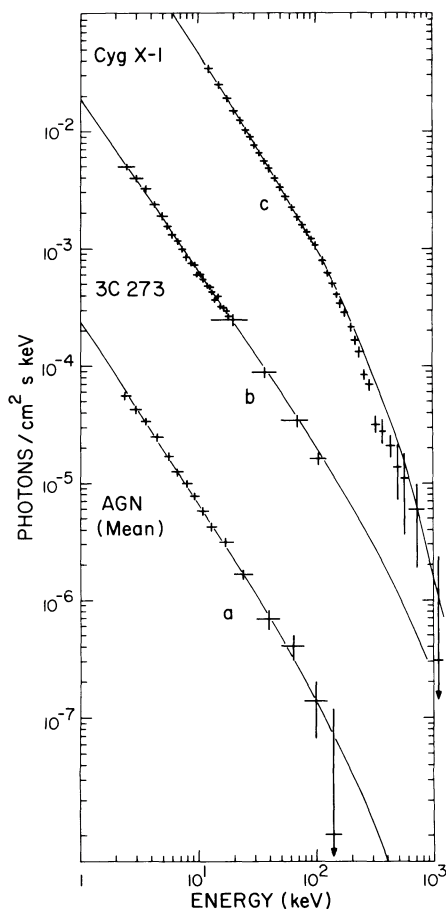


FIG. 3.—Visual fits (not optimized) for different sources. (a) the *HEAO 1* mean AGN spectrum (Rothschild *et al.* 1983), with a superposed theoretical curve for  $kT_{\max} = 237$  keV. (b) The 3C 273 data from *HEAO A-2* (Worrall *et al.* 1979) and *HEAO A-4* (Primini *et al.* 1979), with a superposed theoretical curve of  $kT_{\max} = 511$  keV. (c) The Cyg X-1 data from *HEAO 1* (Rothschild 1981), with a superposed theoretical curve of  $kT_{\max} = 237$  keV. The points falling below the curve in the region 250–500 keV could possibly be associated with redshifted  $e^+e^-$  effects.

detected at about 560, 720, and 1100 keV. There are five observed points between about 250 keV and 500 keV which appear to fall somewhat below the theoretical curve. This may or may not be real, but if it is, it would suggest some type of absorption process, perhaps related to the redshifted 511 keV  $e^+e^-$  pair formation feature (see also Nolan and Matteson 1983). If the rest is a continuum, one may say that the fit to this between 10 and 1100 keV is very good.

What are the implications of this for accreting black hole models? It is clear that good fits may be obtained with this method for other objects as well, besides the three considered above. The theoretical curves of Figure

2 span a range of indices from about 1.2 to about 2.2, comparable to the observed range (e.g., Mushotzky 1983). The canonical observed value 1.65 can be interpreted in terms of an expected  $kT_{\max}$  near 200–250 keV in the Mészáros and Ostriker (1983) model. The somewhat higher value required by 3C 273 may be due to an intrinsically higher luminosity. If this interpretation is correct, one would expect sources accreting closer to  $10^{-1} M_{\text{Edd}}$  to have, in general, a harder slope than those at  $\dot{M} \ll 10^{-1} M_{\text{Edd}}$ . Above about  $10^{-1} M_{\text{Edd}}$ , Comptonization would have to be considered, which may further harden the index.

It should be stressed that good fits can also be obtained with some other models. Synchro-Compton models of X-ray AGNs have been made by, among others, Grindlay (1975) and Mushotzky *et al.* (1978). Some conceptual difficulties remain, such as inconsistent X-ray to radio luminosity and time variability ratios (Halpern and Grindlay 1983; Schwartz and Ku 1983). Comptonization models of AGNs were considered by Katz (1976), Lightman and Rybicki (1979), and Sunyaev and Titarchuk (1980). Comptonization models for Cyg X-1 were calculated by, e.g., Shapiro, Lightman, and Eardley (1976) and Sunyaev and Trümper (1979) (see also Nolan and Matteson 1983), producing very good fits. The main conceptual difficulty (cf. Lightman 1981) is to understand why the spectral slope varies so little from object to object, since a large spread of  $T_e$  and  $\tau_e$  might be expected, and the values used to achieve the fit are not specifically predicted by the models. The other problem is that changes of  $L_x$  (or  $\dot{M}$ ) would change  $\tau_T$  and perhaps  $T_e$ , which would change the slope; this correlation, however, is not observed (e.g., Mushotzky 1983). While none of these difficulties with synchro-Compton and Compton models are fatal, they emphasize the fact that the simple thermal models discussed here should be considered seriously, since they are free of some of these difficulties. In spherical bremsstrahlung models, the slope depends on  $T_{\max}$ , but for  $h\nu \lesssim 0.5 kT_{\max}$  only weakly so, and in the Mészáros and Ostriker (1983) model,  $\langle h\nu_e \rangle \sim 0.25 kT_{\max}$  is very insensitive to changes in  $\dot{M}$ , since, below the shock, the Comptonization is saturated. Furthermore, it is remarkable that these models seem to fit very well a wide range of observed objects, with a minimum of parameters whose value can be reasonably justified from the model itself. On the other hand, jets, high-polarization, and/or radio emission, which occur in less than 10%–20% of all sources, are probably easier to produce in other, nonspherical models (e.g., disks). We can conclude that thermal emission from spherical infall may account for the X-ray luminosity of the larger fraction of radio-quiet, unpolarized quasars, AGNs, and galactic black holes.

## REFERENCES

- Cowie, L. L., Ostriker, J. P., and Stark, A. A. 1978, *Ap. J.*, **226**, 1041.  
 Gluckstern, R. L., *et al.* 1953, USAEC Report AECD-4246 (Yale [LA]3).  
 Görecki, A., and Kluzniak, W. 1981, *Acta Astr.*, **31**, 457.  
 Grindlay, J. E. 1975, *Ap. J.*, **199**, 49.  
 Halpern, J. P., and Grindlay, J. E. 1983, *Nature*, in press.  
 Ipser, J. R., and Price, R. H. 1982, *Ap. J.*, **255**, 654.



- Katz, J. I. 1976, *Ap. J.*, **206**, 910.  
 Kylafis, N. D., and Lamb, D. Q. 1982, *Ap. J. Suppl.*, **48**, 239.  
 Lightman, A. P. 1981, in *X-Ray Astronomy in the 1980's*, ed. S. S. Holt (NASA Technical Memorandum 83848; Washington, D.C.: GPO).  
 Lightman, A. P., and Rybicki, G. 1979, *Ap. J. (Letters)*, **229**, L15.  
 Maraschi, L., Perola, G. C., Reina, C., and Treves, A. 1979, *Ap. J.*, **230**, 243.  
 Maxon, S. 1972, *Phys. Rev. A*, **5**, 1630.  
 Mészáros, P. 1975, *Astr. Ap.*, **44**, 59.  
 Mészáros, P., and Ostriker, J. P. 1983, *Ap. J. (Letters)*, **273**, L59.  
 Mészáros, P., and Silk, J. I. 1977, *Astr. Ap.*, **55**, 289.  
 Mushotzky, R. F., Serlemitsos, P. J., Becker, R. H., Boldt, E. A., and Holt, S. S. 1978, *Ap. J.*, **220**, 790.  
 Mushotzky, R. G. 1983, in *Proceedings of the Eleventh Texas Symposium on Relativistic Astrophysics*, *Ann. NY Acad. Sci.*, in press.  
 Nolan, P. L., and Matteson, J. L. 1983, *Ap. J.*, **265**, 389.  
 Ostriker, J. P., McCray, R., Weaver, R., and Yahil, A. 1976, *Ap. J. (Letters)*, **208**, L61.  
 Primini, F. A., et al. 1979, *Nature*, **278**, 234.  
 Quigg, C. 1968*a*, *Ap. J.*, **151**, 1187.  
 \_\_\_\_\_ 1968*b*, *Phys. Fluids*, **11**, 461.  
 Rothschild, R. E., Mushotsky, R. F., Baity, W. A., Gruber, D. E., Matteson, J. L., and Peterson, L. E. 1983, *Ap. J.*, **269**, 423.  
 Rothschild, R. E. 1981, in *X-Ray Astronomy in the 1980's*, ed. S. S. Holt (NASA Technical Memorandum 83848; Washington, D.C.: GPO).  
 Schwartz, D. A., and Ku, W. H.-M. 1983, *Ap. J.*, **266**, 459.  
 Shapiro, S. L., Lightman, A. P., and Eardley, D. M. 1976, *Ap. J.*, **204**, 187.  
 Sunyaev, R. A., and Titarchuk, L. G. 1980, *Astr. Ap.*, **86**, 121.  
 Sunyaev, R. A., and Trümper, J. 1979, *Nature*, **279**, 506.  
 Worrall, D. M., Mushotsky, R. F., Boldt, E. A., Holt, S. S., and Serlemitsos, P. J. 1979, *Ap. J.*, **232**, 683.  
 Zdziarski, A. A. 1983, *Acta Astr.*, in press.

PETER MÉSZÁROS: Harvard-Smithsonian Center for Astrophysics, 60 Garden Street, Cambridge, MA 02138